

# Solid-Liquid Transition in a Skyrmion Matter

Dmitry A. Garanin and Eugene M. Chudnovsky

*Physics Department, Herbert H. Lehman College and Graduate School, The City University of New York,  
250 Bedford Park Boulevard West, Bronx, New York 10468-1589, USA*

(Dated: March 4, 2024)

We report Monte-Carlo studies of the orientational order and melting of a 2D skyrmion lattice containing more than one million spins. Two models have been investigated, a microscopic model of lattice spins with Dzyaloshinskii-Moriya interaction that possesses skyrmions, and the model in which skyrmions are treated as point particles with repulsive interaction derived from a spin model. They produce similar results. The skyrmion lattice exhibits a sharp one-step transition between solid and liquid phases on temperature and the magnetic field. This solid-liquid transition is characterized by the kink in the magnetization. The field-temperature phase diagram is computed. We show that the application of the field gradient to a 2D system of skyrmions produces a solid-liquid interface that must be possible to observe in experiments.

## I. INTRODUCTION

Skyrmions [1] have been among the most studied objects in magnetic systems in recent years due to their potential for developing topologically protected nanoscale information carriers [2–6]. In materials lacking inversion symmetry, individual skyrmions are usually stabilized by Dzyaloshinskii-Moriya interaction (DMI) [7–12]. Frustrated exchange interactions [13, 14], magnetic anisotropy [15, 16], disorder [17], and geometrical confinement [18] provide additional mechanisms for the stabilization of skyrmions.

Bogdanov and Hubert [8] pioneered studies of two-dimensional (2D) lattices of magnetic vortices in systems with DMI. They obtained the magnetic phase diagram separating periodic arrangements of vortices from laminar domains. Skyrmion lattices were initially observed by the real-space Lorentz transmission electron microscopy [19] in FeCoSi films. Many studies that followed confirmed reported transitions between uniformly magnetized states, laminar domains, and skyrmion crystals on temperature and the magnetic field, see, e.g., Refs. [20, 21], and references therein.

More recently, it was realized that skyrmion lattices provide a new area for the studies of 2D melting [22–25]. This general problem of statistical physics emerged in the 1970s with the seminal works of Kosterlitz and Thouless [26], Halperin and Nelson [27, 28], and Young [29] (see Ref. [30] for an early review). It was proposed that, in line with the Kosterlitz-Thouless theory of 2D melting, a 2D solid melts via unbinding of defects but in a two-step manner via the so-called KTHNY scenario named after the above authors. In that scenario, a 2D solid first undergoes a transition into an intermediate hexatic phase via unbinding of dislocations. It is characterized by the exponential decay of translational correlations and the algebraic decay of orientational correlations. Then, on further warming, it melts into a true liquid state with exponential decay of all correlations via unbinding of disclinations.

These theoretical predictions were confirmed by several numerical studies [31, 32] and in experiments on colloidal

particles [33, 34], see Ref. [35] for review. Nevertheless, the phase diagram of the 2D melting is far from being settled. Early studies that used molecular dynamics [36] emphasized the importance of the competition between long-wave fluctuations, which are particularly important in 2D, and short-wave phonons that can drive a conventional first-order melting in 2D as they do in 3D. Subsequently, it was established that the melting scenario was not universal but depended on the interaction potential [36–38] and the symmetry of the lattice [39, 40].

The debate related to the melting scenario has proliferated into recent studies of skyrmion lattices as well. Monte Carlo simulations of the microscopic spin model by Nishikawa et al. [22] demonstrated a direct melting of the skyrmion lattice into a 2D liquid with short-range correlations as in 3D and no evidence of the intermediate hexatic phase. A similar conclusion was made in our recent Monte-Carlo studies [25] of lattices of up to  $10^5$  skyrmions treated as particles with negative core energy and repulsive interaction obtained from a microscopic spin model [41]. On the contrary, simulations of skyrmion lattices in a  $\text{GaV}_4\text{S}_8$  spinel by Baláz et al. [24] showed a two-step KTHNY melting transition. Such a transition was also reported in experiments on a  $\text{Cu}_2\text{OSeO}_3$  nanoslab by Huang et al. [23] using cryo-Lorentz transmission electron microscopy.

In this paper, we compare the results of Monte Carlo studies of the melting of a skyrmion lattice obtained within a point particles (PP) model, as described above, and also within the underlying microscopic lattice-spins (LS) model. Good agreement between the two models is demonstrated and the single transition is confirmed. It exhibits a kink in the magnetization that provides a convenient tool for experimental detection of melting. We also explore a novel feature of the 2D melting transition in skyrmion lattices that is absent in atomic systems. Unlike a 2D atomic monolayer, the skyrmion lattice can exhibit melting not just on temperature  $T$  at a fixed magnetic field  $H$  but also on changing the field  $H$  at a fixed temperature  $T$ . The  $(T, H)$  phase diagram is computed, which can be tested in experiments. Moreover, non-uniform ordering arises in the presence of the

magnetic-field gradient.

The paper is organized as follows. The theoretical background for the studies of equilibrium skyrmion lattices and the degree of the orientational order in the lattice is given in Sec. II. Numerical methods are described in Sec. III. The temperature dependence of the orientational order parameter is computed in Sec. IV A. Section IV C shows the results for the number of skyrmions in the system at different temperatures, obtained within the LS model. The  $(T, H)$  phase diagram is presented and discussed in Sec. IV D. Non-uniform ordering in the presence of the magnetic-field gradient is studied in Sec. IV E. Finally, Sec. V contains concluding remarks and suggestions for the experiment.

## II. THEORY

### A. The model

Our model describes ferromagnetically coupled three-component classical spin vectors  $\mathbf{s}_i$  of length 1 on a square lattice with the energy given by

$$\mathcal{H} = -\frac{1}{2} \sum_{ij} J_{ij} \mathbf{s}_i \cdot \mathbf{s}_j - H \sum_i s_{iz} - A \sum_i [(\mathbf{s}_i \times \mathbf{s}_{i+\delta_x})_x + (\mathbf{s}_i \times \mathbf{s}_{i+\delta_y})_y]. \quad (1)$$

The nearest neighbors exchange interaction of strength  $J > 0$  favors ferromagnetic ordering and incorporates the actual length of the spin. The stabilizing field  $H$  in the second (Zeeman) term is applied in the negative  $z$ -direction,  $H < 0$ . The third term in Eq. (1) is the Dzyaloshinskii-Moriya interaction (DMI) of the Bloch type of strength  $A$ , with  $\delta_x$  and  $\delta_y$  referring to the next nearest lattice site in the positive  $x$  or  $y$  direction. In this configuration, the dominant direction of spins is down and that in the skyrmions is up. The DMI of the Néel type is described by the term  $(\mathbf{s}_i \times \mathbf{s}_{i+\delta_x})_y - (\mathbf{s}_i \times \mathbf{s}_{i+\delta_y})_x$  and leads to the same results.

The spin field in 2D is characterized by the topological charge [1]

$$Q = \int \frac{dxdy}{4\pi} \mathbf{s} \cdot \frac{\partial \mathbf{s}}{\partial x} \times \frac{\partial \mathbf{s}}{\partial y} \quad (2)$$

that takes quantized values  $Q = 0, \pm 1, \pm 2, \dots$ . For the pure-exchange model, the analytical solution for topological configurations with a given value of  $Q$  was found by Belavin and Polyakov [1] (see also Ref. [41]). Skyrmions and antiskyrmions correspond to  $Q = \pm 1$ . Due to the scale invariance of the exchange interaction in 2D, their energy with respect to the uniform state,  $\Delta E_{\text{BP}} = 4\pi J$ , does not depend on their size  $\lambda$ . In a continuous spin-field model, the conservation of the topological charge prevents skyrmions from decaying. Finite lattice spacing  $a$  breaks this invariance by adding a term of the order

$-(a/\lambda)^2$  to the energy, which leads to the skyrmion collapse [42]. This result was generalized for topological structures with any  $Q$  in Ref. [43].

In the presence of the DMI, only skyrmions, but not antiskyrmions, exist. To find a single-skyrmion spin configuration numerically, one can start with any state with  $Q = 1$  and perform energy minimization as described in Ref. [44]. The energy of a single skyrmion with respect to the uniform ferromagnetic state becomes negative for  $A$  large enough and  $|H|$  small enough, making the uniform state unstable to the creation of skyrmions. However, skyrmions compete with the laminar domains. A stable skyrmion solution exists in the field interval  $H_s \leq |H| \leq H_c$ . Below  $H_s \simeq 0.55A^2/J$  skyrmions become unstable against converting into a laminar domain structure [25]. Above  $H_c \simeq 0.97A^{3/2}/J^{1/2}$  skyrmions collapse [44]. The ratio of these fields is  $H_c/H_s \simeq 1.76(J/A)^{1/2}$ . In practice,  $A < J$ , thus providing a finite field range for the existence of skyrmions.

### B. Skyrmion-skyrmion interaction and the skyrmion-lattice parameter

In sufficiently dense skyrmion lattices that we study here, the short-range repulsion between skyrmions is dominating, whereas their dipole-dipole repulsion can be neglected [41]. The former is given by

$$U(d) \simeq F \exp\left(-\frac{d}{\delta_H}\right), \quad F \equiv 60J \left(\frac{A^2}{JH}\right)^2, \quad (3)$$

where  $d$  is the distance between the skyrmions' centers and  $\delta_H = a\sqrt{J/|H|}$  is the magnetic length. This formula offers an alternative (to the LS model) way of building a skyrmion lattice as a system of particles with a repulsive interaction (3). In this paper, we use both methods to describe the melting of skyrmion lattices and compare the results with each other.

The number of skyrmions  $N_S$  in the system at  $T = 0$  can be found from the minimization of the total energy. For a triangular lattice of skyrmions of the period  $a_S$  and total area  $S$

$$N_S = \frac{2}{\sqrt{3}} \frac{S}{a_S^2}. \quad (4)$$

Each skyrmion in the lattice interacts with its six nearest neighbors, whereas interaction with further neighbors is negligibly small. The energy per skyrmion is

$$E_0 = \Delta E + 3F \exp\left(-\frac{a_S}{\delta_H}\right), \quad (5)$$

where  $\Delta E < 0$  is the skyrmion's core energy computed from the LS model [25]. The equilibrium state at  $T = 0$  can be obtained by the minimization of the total energy,  $\mathcal{E} = N_S E_0$  with respect to  $a_S$ , as described in Ref. [25].

For  $A/J = 0.2$  (that is used throughout the paper) and  $H/J = -0.025$  one has  $\Delta E = -4.23J$ ,  $\delta_H = 6.32a$ , and

$F = 154J$  that results in  $a_S = 38.5a$ . The interaction energy between nearest neighbors  $U_0 = F \exp(-a_S/\delta_H) = 0.349J$  defines the scale for the melting temperature that appears to be  $T_m \simeq 0.12J$ .

One can extend the theory, at least qualitatively, by minimizing the free energy  $\mathcal{F} = \mathcal{E} - T\mathcal{S}$ , where  $\mathcal{S}$  is the entropy,

$$\mathcal{S} = N_S \ln \mathcal{N}_{\text{positions}}, \quad (6)$$

and  $\mathcal{N}_{\text{positions}}$  is the number of positions available for skyrmions taking into account their repulsion. At the temperature  $T$  the minimal distance  $r_T$  between skyrmions can be estimated as  $F e^{-r_T/\delta_H} \simeq T$  that results in

$$r_T \simeq \delta_H \ln \frac{F}{T}, \quad \mathcal{N}_{\text{positions}} \simeq \frac{S}{r_T^2} = \frac{S}{\delta_H^2} \frac{1}{\ln(F/T)}. \quad (7)$$

Substituting this into the free energy  $\mathcal{F}$  and using Eq. (4), one obtains

$$\mathcal{F} = \frac{2}{\sqrt{3}} \frac{S}{a_S^2} \left[ \Delta E - T \ln \left( \frac{S}{\delta_H^2} \frac{1}{\ln(F/T)} \right) + 3F \exp \left( -\frac{a_S}{\delta_H} \right) \right]. \quad (8)$$

This can be minimized numerically with respect to  $a_S$ , then the number of skyrmions can be found from Eq. (4). The resulting dependence  $N_S(T)$  shown in black in Fig. 9 below is very close to a straight line.

### C. Skyrmion lattice

The positions of skyrmions in a triangular lattice are given by

$$\frac{\mathbf{R}}{a_S} = \mathbf{e}_x n_x + \mathbf{e}_{60} n_{60} = \mathbf{e}_x \left( n_x + \frac{1}{2} n_{60} \right) + \mathbf{e}_y \frac{\sqrt{3}}{2} n_{60}, \quad (9)$$

where  $\mathbf{e}_x$  and  $\mathbf{e}_y$  are unit vectors along  $x, y$  coordinate axes,  $\mathbf{e}_{60} = (1/2)\mathbf{e}_x + (\sqrt{3}/2)\mathbf{e}_y$  is the lattice vector directed at  $60^\circ$  to the  $x$ -axis and  $n_x, n_{60}$ , are integers. We use the value of  $a_S$  obtained by the energy minimization. The regions of  $n_x, n_{60}$  and the dimensions of the system are chosen to avoid distortions of the lattice near the boundaries in the case of periodic boundary conditions (pbc). An example of the initial state used for obtaining the skyrmion lattice within the model of lattice spins is shown in Fig. 1. It consists of Bloch-type bubbles placed in positions given by Eq. 9. Energy minimization at  $T = 0$  results in the skyrmion lattice that for the model with pbc looks similar, except that the size of skyrmions increases [same as for the model with free boundary conditions (pbc) below]. The results for the energy minimization for the fbc model are shown in Fig. 2. Because of the repulsion from the boundary, the lattice is somewhat compressed and distorted near the vertical walls. This effect becomes non-essential in systems of a larger size.

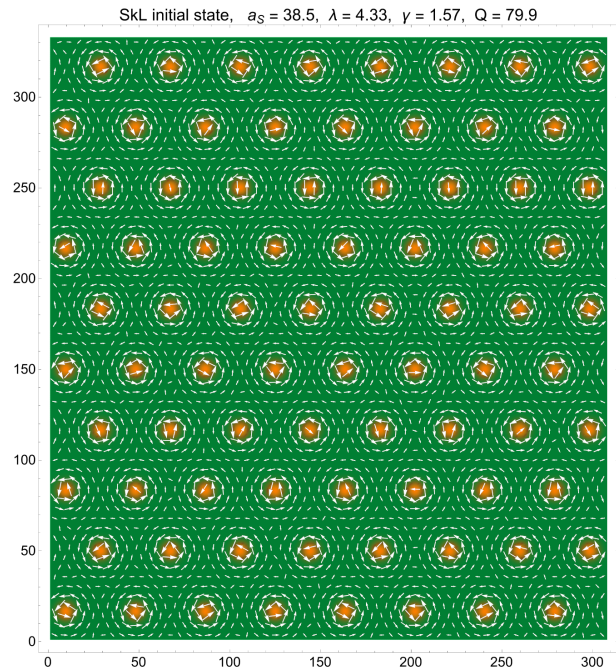


Figure 1. Initial state for the triangular lattice of skyrmions. Spin components are color-coded,  $s_z = -1$  green,  $s_z = 1$  orange. White arrows show the in-plane spin components  $s_x$  and  $s_y$ .

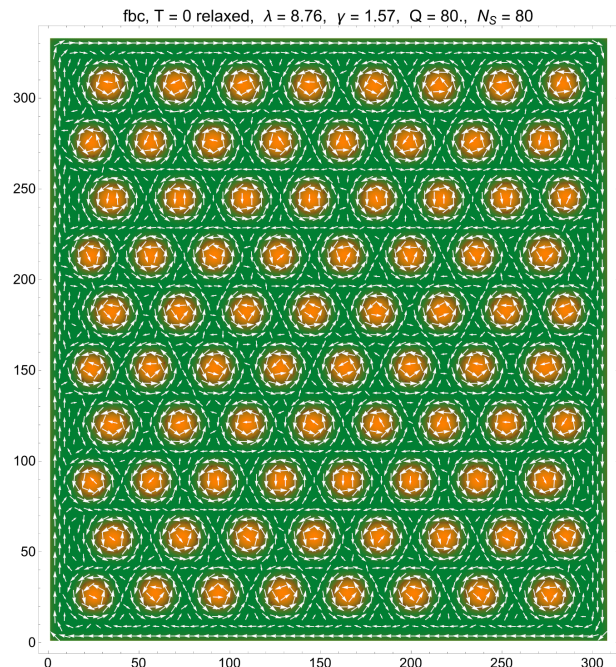


Figure 2. Skyrmion lattice in the lattice-spin model with free boundary conditions obtained through relaxation of the initial state of bubbles with  $Q = 1$ , Fig. 1.

For the model of point particles with repulsion, the particles are initially placed at the positions according to Eq. (9) and then Monte Carlo simulation is performed. For  $T = 0$ , this leads to the energy minimization in general. For the pbc model in this case, the particles remain at their initial positions. The result for the rigid-wall condition at  $T = 0$  is similar to that for the LS model with fbc.

#### D. Orientational order

The quantity describing the orientation of the hexagon of the nearest neighbors of any skyrmion  $i$  in a 2D lattice is local hexagonality

$$\Psi_i = \frac{1}{6} \sum_j \exp(6i\theta_{ij}). \quad (10)$$

Here the summation is carried out over 6 nearest neighbors  $j$ ,  $\theta_{ij}$  is the angle between the  $ij$  bond and any fixed direction in the lattice. If  $\theta$  is counted from the direction of the  $x$ -axis (that is our choice), and two of the sides of the perfect hexagon coincide with the  $x$ -axis (as in the figures above), all terms in the sum are equal to 1, and thus  $\Psi_i = 1$ . We call this *horizontal* orientation of hexagons. Rotation of the hexagons by  $30^\circ$  from the horizontal orientation results in the *vertical* orientation for which  $\Psi_i = -1$ . For any other orientation of a perfect hexagon,  $\Psi_i$  is a complex number of modulus 1. The angle  $\phi_i$  by which the hexagon  $i$  is rotated from its initial horizontal orientation is related to the phase angle  $\Theta_i$  in  $\Psi_i = |\Psi_i| e^{i\Theta_i}$  as  $\phi_i = \Theta_i/6$ .

At finite temperatures, orientations of the bonds fluctuate and the condition  $|\Psi_i| = 1$  no longer holds. The quality of hexagons can be described by global hexagonality value [25] defined as

$$V_6 = \sqrt{\frac{1}{N_S} \sum_i |\Psi_i|^2}, \quad (11)$$

where  $N_S$  is the number of skyrmions in the system. At temperatures well above the melting transition, when even the short-range order is completely destroyed, the orientations of the bonds and the angles  $\theta_{ij}$  become random. In this limit  $V_6 = \sqrt{1/6}$  as each particle has six nearest neighbors on average. The common orientation of hexagons in the lattice is described by the complex order parameter which is defined as local hexagonality averaged over the system:

$$O_6 = \frac{1}{N_S} \sum_i \Psi_i. \quad (12)$$

### III. NUMERICAL METHOD

The lattice-spin model was numerically solved with the help of the energy minimization at  $T = 0$  and by the

Metropolis Monte Carlo routine at  $T > 0$ , as described in Ref. [20]. At  $T = 0$  we applied sequential rotation of spins  $\mathbf{s}_i$  toward their effective field  $\mathbf{H}_{\text{eff},i} = -\partial\mathcal{H}/\partial\mathbf{s}_i$  with the probability  $\alpha$  and the energy-conserving overrelaxation (rotating the spins by  $180^\circ$  around  $\mathbf{H}_{\text{eff},i}$ ) with the probability  $1 - \alpha$ . At  $T > 0$ , we combined the Monte Carlo update and overrelaxation with the same probabilities. In most computations we used  $\alpha = 0.01$  which allows efficient exploring of the phase space of the system by overrelaxation. Monte Carlo updating of all spins in the system constitutes one Monte Carlo step (MCS). We used both lattice initial condition (LIC) and random initial condition (RIC) in which the directions of lattice spins are random. The latter is used to study the freezing of the skyrmion lattice that for large systems leads to a polycrystalline state as different regions freeze with different directions of hexagons and the motion of domain boundaries is very slow below the freezing transition.

We studied the systems of a nearly square shape with dimensions adjusted to the skyrmion lattice with the lattice parameter  $a_S$  computed by the energy minimization as explained above. At the boundaries, we used periodic boundary conditions (pbc) and free boundary conditions (fbc).

To identify skyrmions, we used an adaptation of the well-known algorithm for labeling islands using, as parameters, the *sea level* (the value of  $s_z$  identifying the boundary of the skyrmion's core) equal to zero, *connection range* (the maximal distance between the spins along the  $x$  and  $y$  axes for which they can be considered as neighbors) equal to  $a$  (so that each spin has 8 neighbors), and the *minimal island size* (the number of spins with  $s_z > 0$  in the skyrmion) equal to five. This algorithm checks all spins in the lattice for  $s_z > 0$ . If such spin is found, all its neighbors within the connection range are checked and added to the island if they have  $s_z > 0$ . This ends when there are no more connected neighbors with  $s_z > 0$ . If the number of spins within the island is greater or equal to the minimal island size, the skyrmion is identified. The limitation on the skyrmion size is important at elevated temperatures when spins are substantially disordered and there can be even isolated spins pointing up that should not be counted as skyrmions. After all skyrmions are identified, their centers  $\mathbf{R}_i$  can be found with the help of the skyrmion-locator formula

$$\mathbf{R}_i = \sum_{j \in i} \mathbf{r}_j s_{z,j}^2 / \sum_{j \in i} s_{z,j}^2, \quad (13)$$

where  $j \in i$  are all lattice sites that belong to the skyrmion  $i$ . Here the weight factor  $s_{z,j}^2$  favors the sites close to the skyrmion's top. An example of the skyrmion location is shown in Fig. 3. One can see that at elevated temperatures well above melting, skyrmions are strongly washed out by thermal agitation.

After skyrmions are identified, the system is subdivided into square bins containing 4-6 skyrmions. In the computation of the orientational order, Eqs. (10)-(12), the six nearest neighbors are searched for only within the



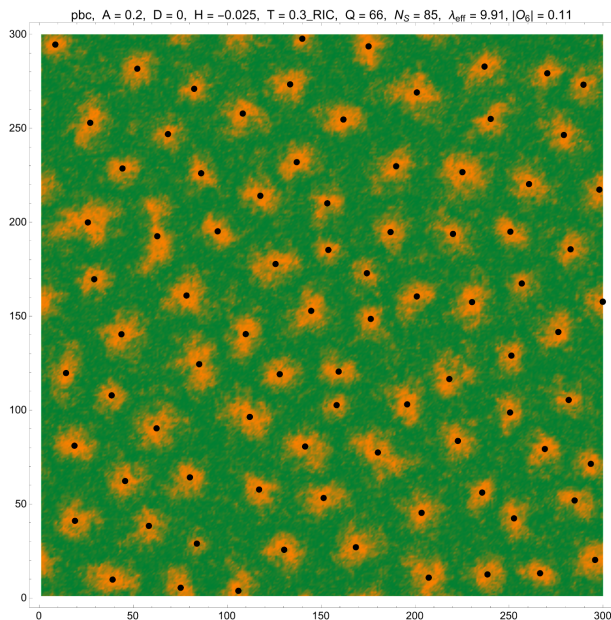


Figure 3. A snapshot of the skyrmion liquid at  $T/J = 0.3$  (above the skyrmion-lattice melting point). Thermal agitation washes out skyrmions' shape. Black points are skyrmions' positions found by the skyrmion locator, Eq. (13).

same bin and the eight surrounding bins. This greatly speeds up the computation.

Computations were performed with Wolfram Mathematica using compilation of the core routines such as the energy minimization and Monte Carlo. We used versions with and without internal parallelization. In the latter, the system is split into the intermittent ABABAB... stripes the number of each of them being equal to the number of used processor cores  $N_{\text{cores}}$ . First, all A-stripes are processed in parallel, then all B-stripes are processed in parallel, and so on. The faster parallelized version was used to study the evolution and the final state of the system at one temperature. To obtain temperature dependences, we used the non-parallelized version computing different temperature points in a parallelized cycle. This works faster than the parallelized version because there is no overhead due to internal parallelization.

The parallelized-cycle computations were done in the so-called *relay* mode in which the next  $T$ -point within the same thread used the previously obtained state as the initial condition. With the interval between the neighboring  $T$ -points being  $\delta T$ , that between those within the same thread was  $\Delta T = N_{\text{cores}} \delta T$  that is sufficiently small if  $\delta T$  is small and  $N_{\text{cores}}$  is not too large.

The largest spin system considered here is about  $1155 \times 1200$  lattice sites which is more than one million spins. For our set of parameters, the perfect skyrmion lattice in this system contains only 1080 skyrmions which is sufficient to observe the melting of the skyrmion lattice and other effects. However, computations with such a large number of spins take a lot of computer time and it is

difficult to scale up the system.

Considering skyrmions as point particles allows performing computations on much larger systems. In Ref. [25] Monte Carlo simulations were done on the systems of up to  $10^5$  particles that showed a first-order phase transition with a narrow  $T$ -hysteresis loop. Here, to compare the LS and PP models, it is sufficient to simulate the systems of  $10^4$  particles. The Metropolis Monte Carlo routine makes successive trial displacements of particles and the trials are accepted if  $\text{rand} < \exp(-\Delta E/T)$ , where  $\text{rand}$  is a random number in the interval (0,1) and  $\Delta E$  is the energy change associated with the trial displacement. The average value of the trial displacement was programmed auto-adjusting to maximize the effective displacement (the average trial displacement times the acceptance rate) and limited from above by  $0.3a_S$ . As in Ref. [25], in computing the repulsion energy, we used the distance cutoff  $r_{\text{cutoff}} = 0.95\sqrt{3}a_S$  that is just shy of the next-nearest distance in the triangular lattice,  $\sqrt{3}a_S$ . The system was subdivided into square bins of a size slightly larger than  $r_{\text{cutoff}}$  so that any particle in the bin could interact with those in the same and eight surrounding bins. With the number of particles 4-6 in the bin, this severely limits the number of interacting partners to consider and greatly speeds up the simulation.

In the Monte Carlo simulation of both LS and PP models, we used the stopping criterion requiring the derivative of a control quantity (CQ) with respect to MCS to be small enough. The CQ was the energy  $U$  per particle in the case of the PP model. For the LS model, we used  $V_6$  given by Eq. (11) as CQ, to put the focus on skyrmions rather than on spins. We averaged the CQ over the last 30% of all MCS' and required  $\Delta \langle \text{CQ} \rangle / (\Delta \text{MCS}) < CQ_{\text{scale}} / \text{MCSens}$ , where  $CQ_{\text{scale}}$  is the scale of the CQ: the interaction energy  $U_0 = F \exp(-a_S/\delta H)$  for  $U$  and 1 for  $V_6$ , while  $\text{MCSens}$  is the sensitivity of the Monte Carlo routine,  $\text{MCSens} = 10^{-7}$  for most simulations. Additionally, we required that the stopping criterion is fulfilled in total for  $10^4$  MCS to exclude a premature stopping in the case the CQ increases and decreases because of fluctuations. Other computed quantities such as  $V_6$  and  $O_6$  were averaged over the last 30% of all MCS', similar to the control quantity. The simulations were performed in blocks of 20 or 50 MCS, to reduce the overhead of computing the system energy or hexagon quality. The number of MCS before stopping was above  $10^5$  in the vicinity of the melting-transition temperature  $T_m$ , smaller above  $T_m$  and even smaller well below  $T_m$ .

Computations were performed on a 20-core Dell Precision workstation with 16 cores licensed for Mathematica, as well as on smaller machines.

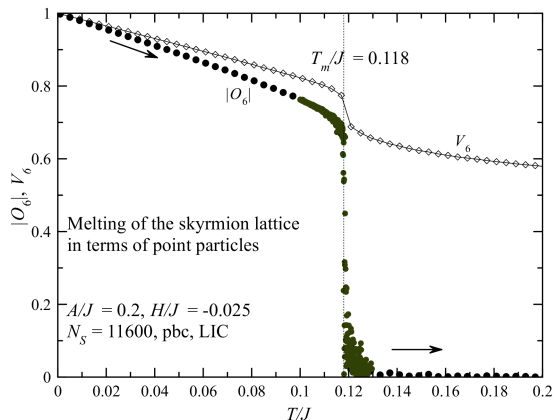


Figure 4. Melting of the skyrmion lattice with periodic boundary conditions in terms of point particles, starting at  $T = 0$  with LIC.

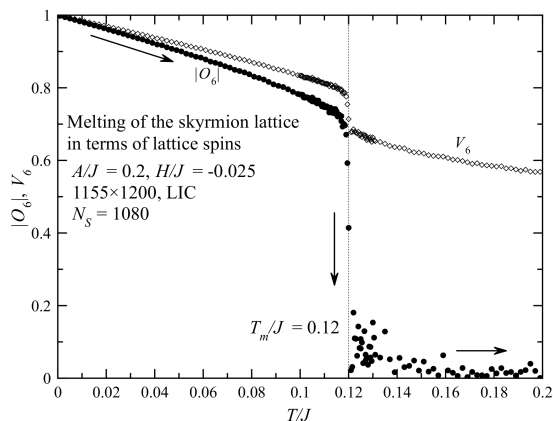


Figure 5. Melting of the skyrmion lattice with periodic boundary conditions in terms of lattice spins, starting at  $T = 0$  with LIC.

## IV. NUMERICAL RESULTS

### A. Melting of the skyrmion lattice

The temperature dependences of the orientational order parameter  $O_6$  and the hexagonality value  $V_6$  for the system of  $10^4$  skyrmions within the point-particle model are shown in Fig. 4. The melting occurs as a single transition at  $T_m = 0.118J$  as in Ref. [25] where a larger system of  $10^5$  particles was simulated. The melting transition is likely first order, although further efforts are needed to fully clarify the critical behavior. The results for the lattice spins model with pbc shown in Fig. 5 are similar, and there is an excellent agreement between the values of  $T_m$  obtained within the two models, despite the number of skyrmions in the LS model is only  $10^3$ .

Free boundary conditions lead to the breakdown of the skyrmion lattice well below the melting transition, as can

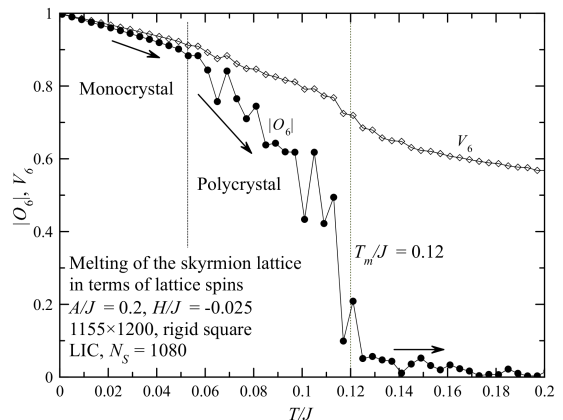


Figure 6. Melting of the skyrmion lattice with free boundary conditions in terms of lattice spins, starting at  $T = 0$  with LIC. Flat boundaries favor the orientation of hexagons parallel to the boundary. This results into breaking an initially monocrystalline skyrmion lattice into a polycrystalline state with the orientation of hexagons defined by the closest boundary. This leads to an irregular dependence  $|O_6(T)|$ .

be seen in Fig. 6 showing the results for the LS model. As was observed in Ref. [25], boundaries polarize the skyrmion solid favoring the orientation of hexagons parallel to the boundary. This effect is the strongest for the system of rhomboid shape in which all boundaries work in the same direction which results in a significant finite-size effect inducing a non-zero  $O_6$  above the melting point. The system of a square shape is frustrated since the horizontal and vertical boundaries work in different directions. As a result, the initially prepared perfect skyrmion lattice with increasing temperature breaks up into a polycrystal in which the boundaries dictate the orientation of hexagons in their vicinity, see Fig. 7. Similar results are obtained for the PP system of a square shape with the rigid-wall boundary conditions.

### B. The magnetization anomaly

As we have seen, most of the results about the skyrmion lattice can be obtained from the point-particle model which is computationally less demanding than the model of lattice spins and allows simulation of larger systems. However, the LS model shows an interesting kink anomaly of the magnetization at the melting point that can be used to locate the melting transition as the magnetization can be measured with great precision. Fig. 8 shows an expected linear decrease of the magnitude of the magnetization  $\mathbf{m} = (1/N) \sum_i \langle \mathbf{s}_i \rangle$  with increasing temperature and, on the top of it, a sudden increase of it in the narrow region of melting.

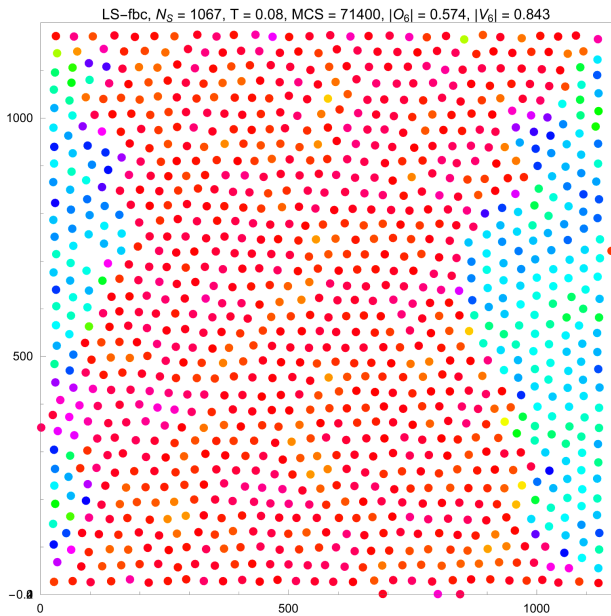


Figure 7. The polycrystal state of the skyrmion lattice in the lattice-spins system with free boundary conditions at  $T/J = 0.08$ . Boundaries favor the orientation of hexagons (color coded) parallel to the boundary. The initial state is a lattice with the horizontal hexagon orientation (red).

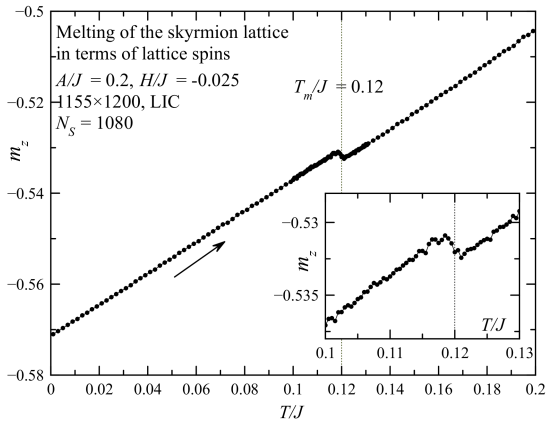


Figure 8. Temperature dependence of the magnetization shows a kink at the melting point.

### C. The number of skyrmions

The equilibrium number of skyrmions  $N_S$  discussed in Sec. II B is, in fact, a complicated issue because at low temperatures  $N_S$  is very difficult to change. Creation of a skyrmion requires overcoming an energy barrier only slightly lower than  $4\pi J$  (see Ref. [44] for details). Annihilation of a skyrmion with a negative energy  $\Delta E$  requires overcoming of an even larger barrier. In the region of the melting,  $T \sim 0.1J$ , the probability of these processes is exponentially small which makes them hardly accessible

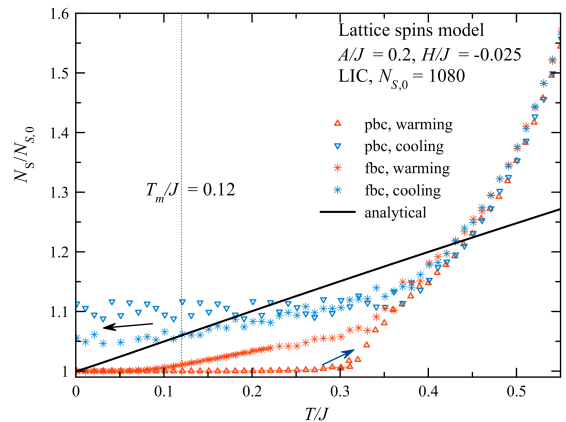


Figure 9. Temperature dependence of the number of skyrmions in the model of lattice spins. In the pbc model,  $N_S$  barely changes below  $T/J = 0.3$ . In the fbc model, there is some increase due to the creation of skyrmions in the cracks between crystallites on the polycrystalline state. Both dependences have a hysteresis. The black line in the result of the numerical minimization of the free energy, Eq. (8).

to Monte Carlo simulations. In the experiment, however, the situation can be different because there is a huge factor between real time and computer time so an exceedingly long computation can correspond to a short real time. In any case, changing of the number of skyrmions in the system is a slow process because within the continuous approximation, skyrmions are topologically protected and the topological charge  $Q$  of the system can change only via the lattice-mediated processes [42].

Treating skyrmions as point particles in Monte Carlo simulations allows for bypassing the barrier of the skyrmion creation/annihilation. However, for our set of parameters, removing a skyrmion from a lattice costs the energy  $2.14J$  while adding a skyrmion into a lattice lacuna costs the energy  $9.89J$  [25]. Although these energies are smaller than  $4\pi J$ , they are large enough to prevent equilibration of the number of skyrmions below melting with the help of a Monte Carlo simulation, if it were extended to include C/A processes.

The results obtained for the lattice-spins model with pbc (in which the number of skyrmions is not fixed and can change naturally) are shown in Fig. 9. For the model with pbc containing  $N_{S,0} = 1080$  skyrmions in LIC at  $T = 0$ , on increasing the temperature  $N_S$  starts to grow only at  $T/J \simeq 0.3$  and then goes up steeply. On cooling,  $N_S$  does not fully return to its initial value, so that  $N_S/N_{S,0} \simeq 1.1$  at low temperatures. The number of skyrmions becomes non-equilibrium below  $T/J \simeq 0.4$  in this simulation.

For the LS model with fbc the results are similar except for the growth of  $N_S$  that starts already at  $T/J \simeq 0.1$ . This can be attributed to the boundaries between domains with different orientations of hexagons in the polycrystal lattice (see Fig. 7) where the lattice is broken and

it should be easier to create or annihilate skyrmions. The massive growth of  $N_S$  starts, however, only at  $T/J \simeq 0.3$ , as in the model with pbc. The fbc model also shows a hysteresis, although weaker than the pbc model.

In Fig. 9, the analytical result for the number of skyrmions following from the minimization of the free energy, Eq. (8) is shown by the black line that is almost straight and different from the numerical results for the LS model with pbc and fbc. The lack of agreement can be explained by the two factors. First, Monte Carlo results at low temperatures are non-equilibrium with respect to  $N_S$ . Second, at elevated temperatures, the model of point particles cannot be quantitatively correct because skyrmions are strongly distorted by thermal fluctuations (see Fig. 3).

#### D. Phase diagram

Unlike the system of particles, the system of skyrmions can show the melting transition not only on temperature  $T$  but also on the magnetic field  $H$ . The latter dependence comes both from the dependence of the magnetic-field length  $\delta H$ , defined below Eq. (3), and from the dependence of the skyrmion's core energy  $\Delta E(H)$  that can be computed from the lattice-spins model. Assuming the concentration of skyrmions in the system to be equal to their equilibrium concentration at  $T = 0$  found in Sec. II B, one can compute the  $(H, T)$  phase diagram by increasing the temperature from zero for each value of  $H$ , performing the Monte Carlo simulation, and detecting the melting temperature  $T_m$ . The results of such computation for a small point-particle system with  $N_S = 1080$  and pbc are shown in Fig. 10 together with the skyrmion-skyrmion repulsion energy  $U_0$ . The same data is shown in Fig. 11 which gives the idea of the values of  $|O_6(H, T)|$ .

As pointed out above, the number of skyrmions in the system is difficult to change at low temperatures including the region of the melting of the skyrmion lattice. With  $N_S$  decoupled from the other parameters, one has to consider the three-parameter phase diagram  $(H, T, N_S)$ . Leaving this task for now, one can produce  $(H, T)$  diagrams with  $N_S$  fixed. Fig. 12 shows the latter for the two values of the skyrmion concentration corresponding to the equilibrium at  $T = 0$  and the two different values of the magnetic field  $H_0$  computed via the minimization of the energy in Sec. II B. Here, the skyrmion lattice exists also in the region to the right of the vertical dotted line where the skyrmion's core energy  $\Delta E$  is positive and skyrmions are metastable. At  $|H|/J = 0.034$  skyrmions collapse.

#### E. Skyrmion lattice in the gradient magnetic field

The influence of the magnetic field on skyrmions is impressively demonstrated by the solid-liquid interface caused by the gradient magnetic field, see Fig. 13. For

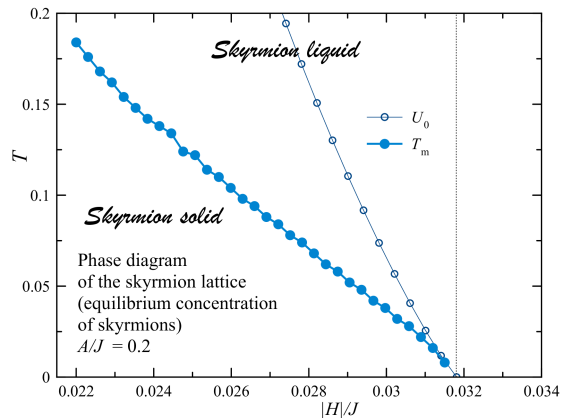


Figure 10. The phase diagram of the skyrmion liquid-solid system assuming the concentration of skyrmions equal to their equilibrium concentration at  $T = 0$  for any value of  $H$ . The melting temperature correlates with the skyrmion-skyrmion repulsion energy  $U_0$  that is also shown.

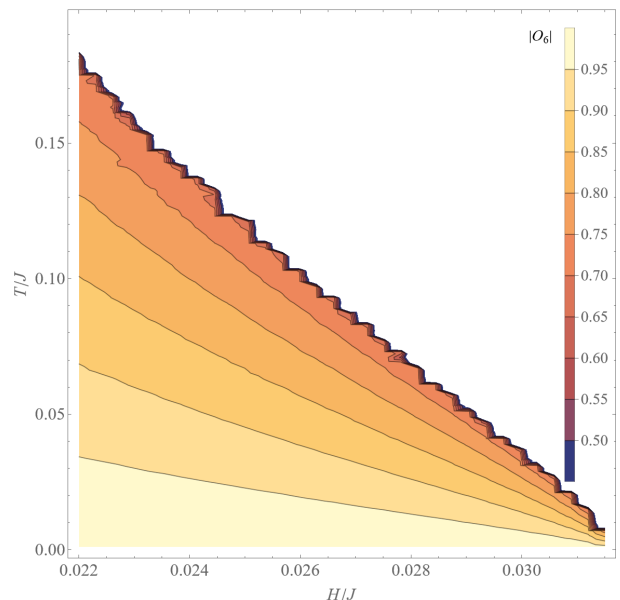


Figure 11. The contour plot showing the magnitude of the orientational order parameter  $O_6(H, T)$ , assuming the concentration of skyrmions equal to their equilibrium concentration at  $T = 0$  for any value of  $H$ .

the temperatures in the vicinity of  $T_m$  applying a field gradient causes phase separation because the melting temperature depends on the magnetic field. We illustrated this phenomenon by applying the maximal possible field gradient so that near the left boundary of the system the field is only a bit stronger than the value at which skyrmions are branching out and give way to the laminar domain structure and near the right boundary the field is only a bit weaker than the skyrmion-collapse field. For  $A/J = 0.2$  the field in the middle of the system



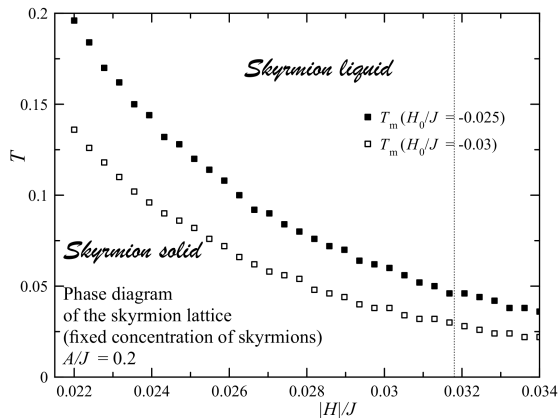


Figure 12. The phase diagram of the skyrmion liquid-solid system for the two values of the concentration of skyrmions equal to their equilibrium concentrations at  $T = 0$  for two different values of  $H$ . Here, for other values of  $H$ , the concentration of skyrmions is non-equilibrium.

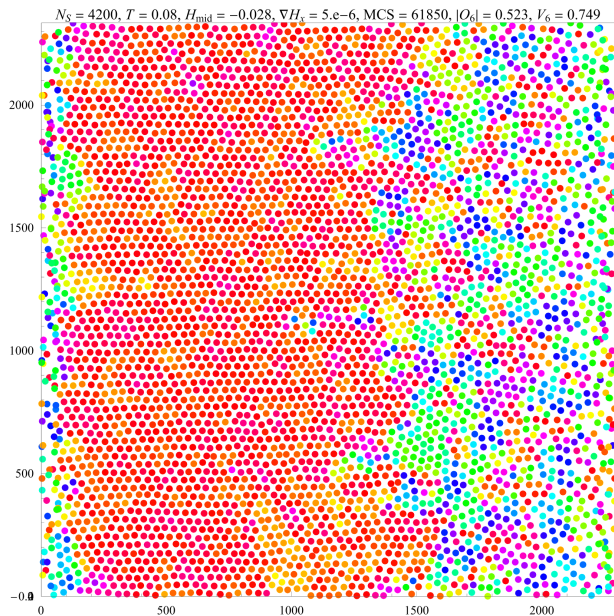


Figure 13. Skyrmion configuration with a solid-liquid interface in the presence of a magnetic-field gradient. On the left, the magnetic field is weaker, the skyrmion repulsion is stronger,  $T_m$  is higher, and at the given temperature the skyrmion lattice holds. On the right, the field is weaker and the lattice melts.

is  $H_{\text{mid}}/J = -0.028$ . For the small system of  $N_S = 4200$  skyrmions shown in Fig. 13 the maximal value of the gradient we used was  $(\partial H_z/dx)(a/J) = 5 \times 10^{-6}$ .

Fig. 14 shows quantitative results for the skyrmion solid-liquid interfaces at different temperatures for a large system of  $N_S = 104400$  skyrmions in the presence of the maximal magnetic-field gradient  $(\partial H_z/dx)(a/J) = 10^{-6}$ . Here, the values of  $|O_6|$  and  $V_6$  are averages over

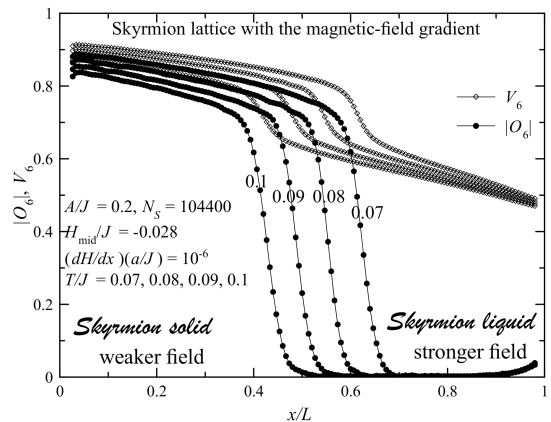


Figure 14. The magnitude of the orientational order parameter  $O_6$  and the hexagonality value  $V_6$  in the presence of a magnetic-field gradient at different temperatures show a solid-liquid interface.

the bins with different  $y$  positions, keeping the  $x$  positions as a parameter.

Both Figs. 13 and 14 were obtained within the point-particle model that allows simulation of large systems of skyrmions.

An interesting question is whether skyrmions would move to the right or to the left if a gradient field is applied. It is known that a gradient field can be used to move skyrmions. Within the PP model, this effect comes from the magnetic-field dependence of the skyrmions core energy,  $\Delta E(H)$ . As  $\Delta E$  is lower for weaker fields, skyrmions would move to this region, on the left in the figures. However, skyrmions also repel each other, and in the region of the weaker field, the repulsion is stronger as the magnetic length defining the skyrmion-skyrmion interaction is longer. Under the action of the increased repulsion, skyrmions would move away from the region of the weaker field. These two competing effects compensate each other so that one cannot see any non-uniform density of skyrmions in Fig. 13. This is a plausible result because the equilibrium concentration of skyrmions that was set in the initial state used to obtain the results above is the result of the balancing between the skyrmion's core energy and their repulsion energy. One can expect that for the concentration of skyrmions lower than the equilibrium one, skyrmions will shift to the left as their repulsion is weaker and the core-energy effect dominates. On the other hand, for the concentration of skyrmions higher than the equilibrium one the repulsion is stronger and makes skyrmions shift to the right.

## V. CONCLUSIONS

We have studied temperature and field dependence of the orientational order in 2D skyrmion lattices developed in the background of over one million lattice spins.

Two complementary approaches have been investigated by the Monte Carlo method, the one in which skyrmions are treated as point particles with repulsive interaction derived from a microscopic model of lattice spins, and the other in which skyrmions are extended objects that emerge in a full microscopic spin model. Excellent agreement between the two models has been found that provides strong confidence in our results.

The long-range ordering in a hexagonal skyrmion lattice is strongly influenced by the shape of the boundary because it favors certain orientations of hexagons and, thus, generates an orientational epitaxy. This, in turn, produces a finite-size effect on the long-range orientational order. The effect is especially strong for a rhomboid shape of the boundary that favors uniform orientation of hexagons and thus a monocrystalline order. On the contrary, the boundary of the square shape generates frustration that forces a monocrystalline hexagonal lattice to break into a polycrystal.

The hexagonal skyrmion lattice is stable in a finite temperature and magnetic field range. At a fixed field, its melting is clearly seen in a step-like drop of the orientational order parameter at a certain temperature that depends on the field. At that temperature, the magnetization of the system exhibits a kink, which provides

an independent tool for detecting the solid-liquid phase transition. At a fixed temperature, the transition can be achieved by increasing the field. We have drawn the temperature-field phase diagrams for different concentrations of skyrmions.

The existence of the solid-liquid phase transition on both temperature and the magnetic field in a 2D skyrmion lattice introduces a new element into the studies of the problem of 2D melting that has been investigated for 50 years. In particular, we observed an interesting behavior when we applied a gradient of the magnetic field to such a system. In the presence of the field gradient, it develops an interface between solid and liquid phases. This may provide another independent tool for observing phases of the skyrmion matter in experiments.

## VI. ACKNOWLEDGMENTS

This work has been supported by the grant No. DE-FG02-93ER45487 funded by the U.S. Department of Energy, Office of Science.

- 
- [1] A. A. Belavin and A. M. Polyakov, Metastable states of two-dimensional isotropic ferromagnets, *Pis'ma Zh. Eksp. Teor. Fiz.* **22** 503–506 (1975) [*JETP Lett.* **22**, 245–247 (1975)]. I, II A, II A
- [2] N. Nagaosa and Y. Tokura, Topological properties and dynamics of magnetic skyrmions, *Nature Nanotechnology* **8**, 899-911 (2013). I
- [3] X. Zhang, M. Ezawa, and Y. Zhou, Magnetic skyrmion logic gates: conversion, duplication and merging of skyrmions, *Scientific Reports* **5**, 9400-(8) (2015).
- [4] G. Finocchio, F. Büttner, R. Tomasello, M. Carpentieri, and M. Klaui, Magnetic skyrmions: from fundamental to applications, *Journal of Physics D: Applied Physics.* **49**, 423001-(17) (2016).
- [5] W. Jiang, G. Chen, K. Liu, J. Zang, S. G. E. te Velthuis, and A. Hoffmann, Skyrmions in magnetic multilayers, *Physics Reports* **704**, 1-49 (2017).
- [6] A. Fert, N. Reyren, and V. Cros, Magnetic skyrmions: advances in physics and potential applications, *Nature Reviews Materials* **2**, 17031-(15) (2017). I
- [7] A. N. Bogdanov and D. A. Yablonskii, Thermodynamically stable “vortices” in magnetically ordered crystals. The mixed state of magnets. *Soviet Physics JETP* **68**, 101-103 (1989). I
- [8] A. Bogdanov and A. Hubert, Thermodynamically stable magnetic vortex states in magnetic crystals, *J. Magn. Mater.* **138**, 255-269 (1994). I
- [9] U. K. Rößler, N. Bogdanov, and C. Pfleiderer, Spontaneous skyrmion ground states in magnetic metals, *Nature* **442**, 797-801 (2006).
- [10] S. Heinze, K. von Bergmann, M. Menzel, J. Brede, A. Kubetzka, R. Wiesendanger, G. Bihlmayer, and S. Blugel, Spontaneous atomic-scale magnetic skyrmion lattice in two dimensions, *Nature Physics* **7**, 713-718 (2011).
- [11] O. Boulle, J. Vogel, H. Yang, S. Pizzini, D. de Souza Chaves, A. Locatelli, T. O. Menten, A. Sala, L. D. Buda-Prejbeanu, O. Klein, M. Belmeguenai, Y. Roussigné, A. Stahkevich, S. M. Chérif, L. Aballe, M. Foerster, M. Chshiev, S. Auffret, I. M. Miron, and G. Gaudin, Room-temperature chiral magnetic skyrmions in ultrathin magnetic nanostructures, *Nature Nanotechnology* **11**, 449-454 (2016).
- [12] A. O. Leonov, T. L. Monchesky, N. Romming, A. Kubetzka, A. N. Bogdanov, and R. Wiesendanger, The properties of isolated chiral skyrmions in thin magnetic films, *New Journal of Physics* **18**, 065003-(16) (2016). I
- [13] A. O. Leonov and M. Mostovoy, Multiply periodic states and isolated skyrmions in an anisotropic frustrated magnet, *Nature Communications* **6**, 8275-(8) (2015). I
- [14] X. Zhang, J. Xia, Y. Zhou, X. Liu, H. Zhang, and M. Ezawa, Skyrmion dynamics in a frustrated ferromagnetic film and current-induced helicity locking-unlocking transition, *Nature Communications* **8** 1717-(10) (2017). I
- [15] B. A. Ivanov, A. Y. Merkulov, V. A. Stepanovich, C. E. Zaspel, Finite energy solitons in highly anisotropic two dimensional ferromagnets, *Physical Review B* **74**, 224422-(17) (2006). I
- [16] S.-Z. Lin and S. Hayami, Ginzburg-Landau theory for skyrmions in inversion-symmetric magnets with competing interactions, *Physical Review B* **93**, 064430-(16) (2016). I
- [17] E. M. Chudnovsky and D. A. Garanin, Skyrmion glass in a 2D Heisenberg ferromagnet with quenched disorder, *New Journal of Physics* **20** 033006-(9) (2018). I

- [18] C. Moutafis, S. Komineas, and J. A. C. Bland, Dynamics and switching processes for magnetic bubbles in nanoelements, *Physical Review B* **79**, 224429-(8) (2009). I
- [19] X. Yu, Y. Onose, N. Kanazawa, J. Park, J. Han, Y. Matsui, N. Nagaosa, and Y. Tokura, Real-space observation of a two-dimensional skyrmion crystal, *Nature* **465**, 901 - 904 (2010). I
- [20] D. A. Garanin, E. M. Chudnovsky, S. Zhang, and X. X. Zhang, Thermal creation of skyrmions in ferromagnetic films with perpendicular anisotropy and Dzyaloshinskii-Moriya interaction, *Journal of Magnetism and Magnetic Materials* **493**, 165724-(9) (2020). I, III
- [21] T. Dohi, R. M. Reeve, and M. Kläui, Thin film skyrmionics, *Annual Review of Condensed Matter Physics* **33**, 73-95 (2022). I
- [22] Y. Nishikawa, K. Hukushima, and W. Krauth, Solid-liquid transition of skyrmions in a two-dimensional chiral magnet, *Physical Review B* **99**, 064435 (2019). I
- [23] P. Huang, T. Schönenberger, M. Cantoni, L. Heinen, A. Magrez, A. Rosch, F. Carbone, and H. M. Rønnow, Melting of a skyrmion lattice to a skyrmion liquid via a hexatic phase, *Nature Nanotechnology* **15**, 761-767 (2020). I
- [24] P. Baláz, M. Paściak, and J. Hlinka, Melting of Néel skyrmion lattice, *Physical Review B* **103**, 174411-(8) (2021). I
- [25] D. A. Garanin and E. M. Chudnovsky, Polyhexatic and polycrystalline states of skyrmion lattices, *Physical Review B* **107**, 014419-(17) (2023). I, II A, II B, II B, II D, III, IV A, IV A, IV C
- [26] J. M. Kosterlitz and D. J. Thouless, Ordering, metastability and phase transitions in two-dimensional systems, *Journal of Physics C: Solid State Physics* **6**, 1181-1203 (1973). I
- [27] B. I. Halperin and D. R. Nelson, Theory of two-dimensional melting, *Physical Review Letters* **41**, 121-124 (1978). I
- [28] D. R. Nelson and B. I. Halperin, Dislocation-mediated melting in two dimensions, *Physical Review B* **19**, 2457-2483 (1979). I
- [29] A. P. Young, Melting and the vector Coulomb gas in two dimensions, *Physical Review B* **19**, 1855-1866 (1979). I
- [30] K. J. Strabburg, Two-dimensional melting, *Review of Modern Physics* **60**, 161-207 (1988). I
- [31] R. Dickman and E. M. Chudnovsky, Elastic lattice in an incommensurate background, *Physical Review B* **51**, 97-106 (1995). I
- [32] Y.-W. Li and M. Pica Ciamara, Accurate determination of the translational correlation function of two-dimensional solids, *Physical Review E* **100**, 062606-(6)(2019). I
- [33] C. A. Murray, W. O. Sprenger, and R. A. Wenk, Comparison of melting in three and two dimensions: Microscopy of colloidal spheres, *Physical Review B* **42**, 688-703 (1990). I
- [34] H. H. von Grünberg, P. Keim, and G. Maret, Phase transitions in two-dimensional colloidal systems, Chapter 2, pp. 40-83 in *Soft Matter, Volume 3: Colloidal Order: Entropic and Surface Forces*, edited by G. Gompper and M. SchickWeinheim : WILEY-VCH, 2007 - ISBN 978-3-527-31370-9. I
- [35] J. M. Kosterlitz, Kosterlitz-Thouless physics: a review of key issues, *Reports on Progress in Physics* **79** 026001-(60) (2016). I
- [36] J. Q. Broughton, G. H. Gilmer, and J. D. Weeks, Molecular-dynamics study of melting in two dimensions: Inverse-twelfth-power interaction, *Physical Review B* **25**, 4651-4669 (1982). I
- [37] E. N. Tsiok, Y. D. Fomin, E. A. Gaiduk, E. E. Tareyeva, V. N. Ryzhov, P. A. Libet, N. A. Dmitryuk, N. P. Kryuchkov, and S. O. Yurchenko, *Journal of Chemical Physics* **156**, 114703-(11) (2022).
- [38] S. C. Kapfer and W. Krauth, *Physical Review Letters* **114**, 035702 (2015). I
- [39] W. Janke and H. Kleinert, From first-order to two continuous melting transitions: Monte Carlo Study of a new 2D lattice-defect model, *Physical Review Letters* **61**, 2344-2347 (1988); Erratum *Physical Review Letters* **62**, 608 (1989). I
- [40] J. Dietel and H. Kleinert, Triangular lattice model of two-dimensional defect melting, *Physical Review B* **73**, 024113 (2006). I
- [41] D. Capic, D. A. Garanin, and E. M. Chudnovsky, Skyrmion-skyrmion interaction in a magnetic film, *Journal of Physics: Condensed Matter* **32**, 415803-(14) (2020). I, II A, II B
- [42] L. Cai, E. M. Chudnovsky, and D. A. Garanin, Collapse of skyrmions in two-dimensional ferromagnets and antiferromagnets, *Physical Review B* **86**, 024429-(4) (2012). II A, IV C
- [43] D. Capic, D. A. Garanin, and E. M. Chudnovsky, Stability of biskyrmions in centrosymmetric magnetic films, *Physical Review B* **100**, 014432 (2019). II A
- [44] A. Derras-Chouk, E. M. Chudnovsky, and D. A. Garanin, Quantum collapse of a magnetic skyrmion, *Physical Review B* **98**, 024423-(9) (2018).

II A, II A, IV C